DOI: 10.1002/chem.200501143

Titanium Phosphonate Porous Materials Constructed from Dendritic Tetraphosphonates

Maxym V. Vasylyev,[a] Ellen J. Wachtel,[b] Ronit Popovitz-Biro,[c] and Ronny Neumann*[a]

Abstract: An organic–inorganic hybrid material, TPPhA-Ti, was constructed by non-hydrolytic condensation of a dendritic tetrakis-1,3,5,7-(4-phosphonatophenyl)adamantane precursor and titanium(IV) isopropoxide. One preparative pathway yielded insoluble materials with a Ti/P ratio of ~1 which was confirmed by a combination of FT-IR, TGA, and EDS measurements. N_2 sorption experiments showed that TPPhA-Ti is a porous solid (micropores ~13 Å; mesopores ~38 Å) with a high surface area, ~550 $m^2 g^{-1}$. The structure and morphology of the TPPhA-Ti as investigated by transmission and scanning electron microscopy showed a layered-type material. Additional X-ray diffraction data suggest a paracrystalline material; an optimization of possible molecular arrangements of TPPhA-Ti was simulated that was in agreement with the experimental data. A second preparative pathway yielded a Ti oxide–phosphonate with a Ti/P ratio of ~3.4. Both TEM and SEM revealed that hollow nanospheres were formed with diameters of ~180–300 nm.

Keywords: dendrimers · layered materials · nanospheres · organic–inorganic hybrid composites · porous materials · titanium phosphonates

Introduction

Synthesis of inorganic–organic hybrid materials is a rapidly growing research area. The continual increase in interest that this field of solid-state chemistry has experienced over the last decade can be explained by the increasing technological need for multifunctional porous materials with numerous useful properties. Synthesis of metal phosphonate materials represents a particularly important direction of research in this area mainly due to the fact that the use of organophosphonate derivatives provides an almost unlimited ability to vary the organic component leading to variable modes of functionalization of the solid material; this also facilitates the control of the pore size.[1] A significant amount of effort has been put into the development of synthetic routes to metal organophosphonates and has resulted in a range of different methods and strategies.[2,3] Many examples of di-, tri- and tetravalent metal organophosphonate compounds have been described; some of them possess ion exchange, catalytic and other properties.[1,4] Recent progress in the preparation and properties of hybrid organic–inorganic materials based on organophosphorous derivatives, including their applications, has been surveyed in recent comprehensive reviews.[1–5]

Layered metal–organic phosphonates constitute a large family of metal phosphonates in which the organic component is situated in between the layers of metal atoms that are covalently bound to the oxygen atoms of the phosphonate groups. When a biphosphonic acid is used, for example biphenylenebis(phosphonate), as the organic component, the metal phosphonate layers become organically pillared; this cross-linking provides additional structural stability to the hybrid material.[2] However, the close proximity of the aryl pillars prevents the formation of a porous material. A way to overcome this close pillar disposition is based on "dilution" of the phosphonate moieties either by the use of biphosphonic acids together with phosphoric, phosphorous or methylphosphonic acid (random pillar separation, low pore size control) or the use of the mixture of 3,3′,5,5′-tetramethylbiphenylenebis(phosphonate) and phosphorous acid (regular pillar separation, narrow pore size distribution).[2,6] Hence, it can be concluded that alkyl or aryl biphosphonic acids used as ditopic building units for the preparation of

[a] M. V. Vasylyev, Prof. Dr. R. Neumann
Department of Organic Chemistry
Weizmann Institute of Science, Rehovot 76100 (Israel)
Fax: (+972) 8-934-4142
E-mail: ronny.neumann@weizmann.ac.il

[b] Dr. E. J. Wachtel
Chemical Research Support Unit
Weizmann Institute of Science, Rehovot, 76100 (Israel)

[c] Dr. R. Popovitz-Biro
Department of Materials and Interfaces
Weizmann Institute of Science, Rehovot 76100 (Israel)

layered metal phosphonates require "dilution" in order to induce interlayer porosity and the necessary increase in bulkiness for better pore size control. On the basis of the above, we thought that the use of tetraphosphonic acid with an extended tetrahedral symmetry, as an example of a polytopic organic building block,[7] could impede the close-packed arrangement of organic molecules in a metal–organic framework. Such an arrangement does permit pore formation and does not require "dilution" with additional building blocks. Since the tetrahedral-shaped adamantane tetrabenzoate (ATB) building unit was successfully used for the assembly of metal–organic frameworks,[7] we decided to synthesize the structurally similar tetrakis-1,3,5,7-(4-phosphonatophenyl)adamantane and to use it in the synthesis of different metal phosphonate hybrid materials.

Thus, as reported in this paper, porous materials can be obtained by a non-hydrolytic condensation of a titanium alkoxide with tetrakis-1,3,5,7-(4-phosphonatophenyl)adamantane that has an extended, rigid tetrahedral configuration. We also show that depending on the solvent used in the condensation reaction, materials of significantly different morphology can be obtained, ranging from layered compounds to hollow nanospheres.

Results and Discussion

Tetrakis-1,3,5,7-(4-phosphonatophenyl)adamantane, TPPhA, was prepared by reacting 1,3,5,7-tetrakis (4-iodophenyl)adamantane and diethylphosphite in a palladium-catalyzed P–C coupling reaction followed by acidic hydrolysis of phosphonic acid diethyl ester as shown in Scheme 1. TPPhA was found to be insoluble in water as well as in all commonly used organic solvents except for DMSO. Therefore, for the preparation of titanium arylphosphonate hybrid material we chose a non-hydrolytic condensation procedure.[3]

Addition of four equivalents of the neat $[(i\mathrm{PrO})_4\mathrm{Ti}]$ to one equivalent of TPPhA dissolved in dry DMSO gave an insoluble white powder which was separated by filtration. The residual DMSO solvent was removed by thorough washing with H_2O, EtOH, and Et_2O followed by drying. The elemental analysis of the tetrakis-1,3,5,7-(4-phosphonatophenyl)adamantine–titanium hybrid material (TPPhA-Ti), was carried out by using energy dispersive X-ray spectroscopic microanalysis (EDS), and provided a Ti/P ratio of ~1:1 measured at various locations on the specimen. Therefore one can conclude that there was compositional homogeneity throughout the hybrid material. In addition, conventional elemental analysis gave C/H/P ratios leading to formulation of a molecular unit as $C_{34}H_{36}O_{12}P_4(TiO_2)_4{\cdot}xH_2O$. The amount of water and the thermal stability of TPPhA-Ti were determined by thermal gravimetric analysis (TGA). The TGA curve shown in Figure 1 demonstrates initial

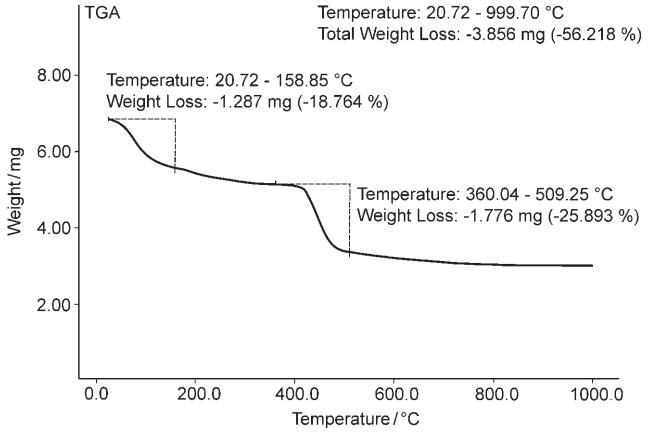

Figure 1. Thermal gravimetric analysis (TGA) curve of TPPhA-Ti hybrid material.

weight loss between 21 and 159 °C attributable to the loss of adsorbed and intercalated water molecules. The water content was calculated from the total weight loss and equals 14 molecules H_2O per formula unit. As can clearly be seen from the TGA curve, thermal decomposition of the organic component of the hybrid material, mainly due to carbon and hydrogen atom extrusion in the form of CO_2, starts at 360 °C and corresponds to 37% of the total weight loss (56%), which is close to the sum of the carbon and hydrogen elements (35.49%) in the unit formula.

The surface–area measurement was based on the five point nitrogen Brenauer–Emmet–Teller (BET) method;[8] TPPhA-Ti exhibited a nitrogen sorption isotherm typical for the mesoporous materials (see Figure 2) with a surface area value of 557 $m^2 g^{-1}$ (Figure 2 inset). The mesopore size distribution curve was derived from the desorption branch of the isotherm by using the Barrett–Joyner–Halenda method;[9] Figure 3 (top) shows the main maximum corresponding to a pore diameter of 38 Å. The total pore volume measured near saturation, $P/P_0 = 0.968$, was 0.42 cc g^{-1}. It was not possible to prepare a nonporous TPPhA-Ti material for the reference nitrogen sorption isotherm measurement required for the relatively accurate de-

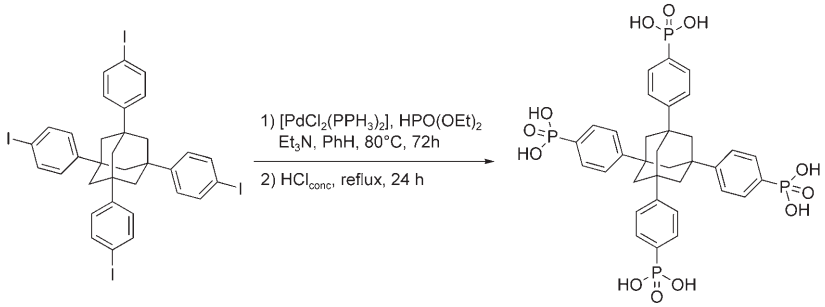

Scheme 1. Synthesis of tetrakis-1,3,5,7-(4-phosphonatophenyl)adamantine (TPPhA).

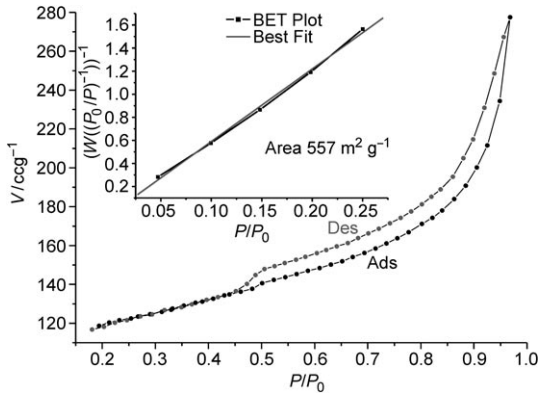

Figure 2. Nitrogen sorption isotherm of TPPhA-Ti hybrid material with a BET plot (inset).

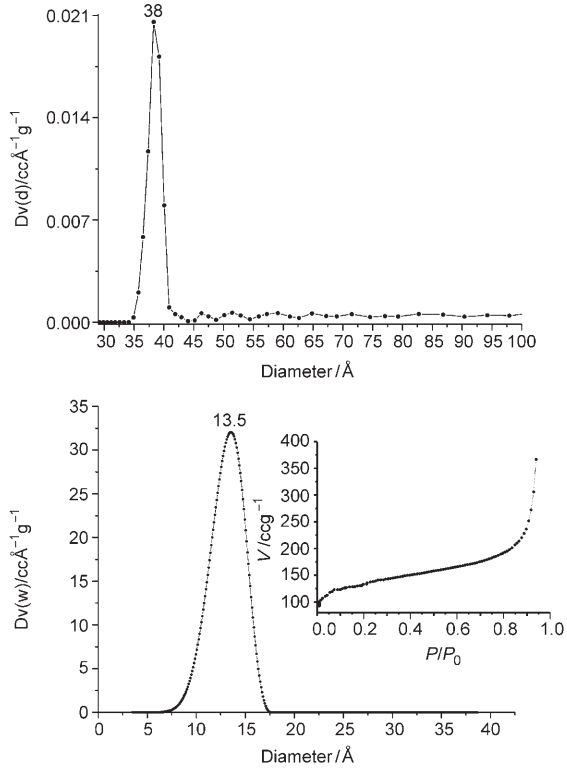

Figure 3. BJH (top) and SF (bottom) pore size distribution curves. Insert on the right is the adsorption isotherm used for the micropore diameter calculation.

termination of the micropore volume in the presence of mesopores by the *T* plot[10] or α_s analysis.[11] Therefore, the micropore size distribution of TPPhA-Ti was derived from the adsorption branch of the isotherm applying Saito–Foley (SF) pore model[12] (Figure 3, bottom). The micropore size distribution curve showed the main maximum corresponding to a pore diameter of 13.5 Å.

Comparison of the FT-IR spectrum of the TPPhA-Ti material obtained with the spectrum of TPPhA as depicted in Figure 4 shows the disappearance of the vibration band at 929 cm^{-1} assigned to P-O···H and the presence of a new band at 1026 cm^{-1} that can be assigned to P-O···Ti vibrations. At the same time the band at 1137 cm^{-1}

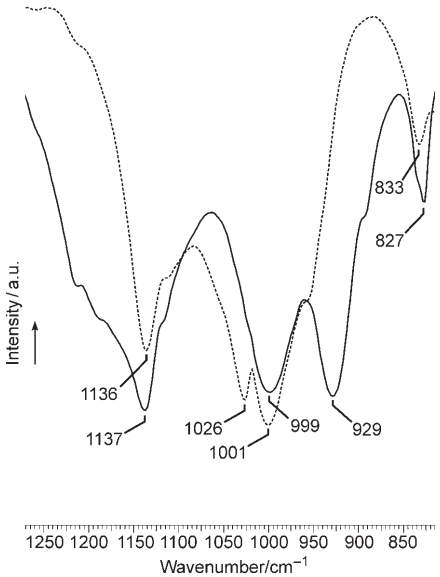

Figure 4. FT-IR spectra of tetrakis-1,3,5,7-(4-phosphonatophenyl)adamantane (solid line) and TPPhA-Ti (dotted line).

(P=O) remained almost unchanged; this implies that the oxygen atom of the P=O fragment does not bind to a titanium atom. This is suggestive of a connectivity, $-P(O)O_2Ti_2O_2(O)P-$ between the phosphonate and titanate moieties as pictured in Scheme 2; this connectivity is supported by the Ti/P ratio obtained by EDS measurements.

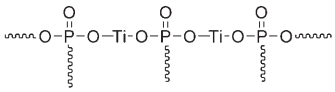

Scheme 2. Proposed connectivity between the phosphonate and titanate moieties.

$^{31}P\{^1H\}$ MAS NMR spectrum of TPPhA-Ti in Figure 5 shows the somewhat broadened resonance signal of the phosphorus nuclei at 13.4 ppm which can be attributed to bidentate phosphonate sites of the $ArP(O)O_2Ti_2O_2(O)PAr$ structural units. The observed ^{31}P chemical shift is similar to the shifts described for the amorphous porphyrin–Zn phos-

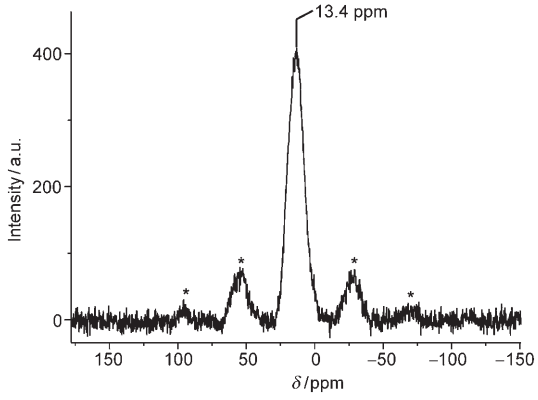

Figure 5. $^{31}P\{^1H\}$ MAS NMR spectrum of TPPhA-Ti. The asterisks denote rotation bands.

phonates[13] and phenylphosphonate–TiO_2 hybrids prepared by the sol–gel method[14] and typical for disordered solids. No sharp ^{31}P NMR resonance signal at -4 ppm, which is claimed to be indicative of a layered titanium phosphonate, was observed.[15]

The X-ray powder diffraction pattern of the TPPhA-Ti hybrid material, Figure 6 (solid line), shows two relatively broad peaks at 2θ values 5.8° (d spacing = 15.2 Å) and 11.2°

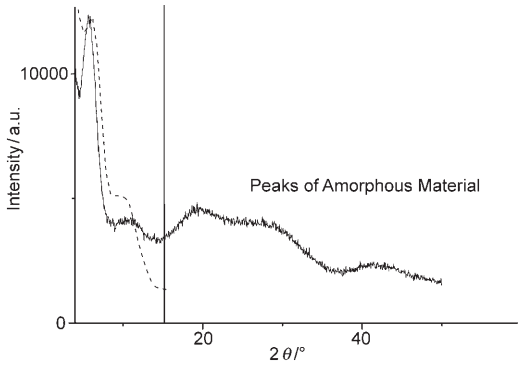

Figure 6. Observed (——) and simulated (-----) X-ray diffraction patterns of TPPhA-Ti hybrid material. The molecular model presented in Figure 8 was used for the simulation.

(d spacing = 7.9 Å) providing some evidence for a weak periodicity. We interpret the presence of three additional diffuse peaks at higher 2θ values as indicating the presence of some amorphous material.

TPPhA-Ti prepared as described above showed two types of morphologies as observed in the typical transmission electron microscope (TEM) images (see Figure 7). One typical morphology shows a layered structure (Figure 7a), as one can more clearly see in the magnified edge area (Figure 7a, inset). One can also observe film-like folded structures (Figure 7b), that are somewhat rolled up at the edges (Figure 7b inset). Attempts to observe a two-dimensional electron diffraction pattern by means of transmission electron microscopy were not successful.

Scanning electron microscopy (SEM) examination of the hybrid TPPhA-Ti material revealed virtually the same type of morphology as observed by TEM (see Figure 8). Plates that have a lamellar structure (Figure 8a and folded films in 8b), with a prevalence of the former were found. In addition to the morphology also seen by TEM, some hemispherical outgrowths (amorphous phase) in the TPPhA-Ti sample were observed in the SEM images (Figure 8c).

By using tetrakis-1,3,5,7-(4-phosphonatophenyl)adamantane as a building block in the synthesis of titanium phosphonate we did not expect the formation of an organically pillared layered material similar to those obtained from the aryl biphosphonic acids.[2,6] The rigid extended tetrahedral structure of TPPhA cannot adopt a conformation in which the phosphonate group tetrahedra will have their oxygen atom bases arranged nearly parallel to the metal layer as is usually observed for the aryl biphosphonic acids.[2,3,6] We believe that molecular units of TPPhA are connected through the titanium atoms with no metal oxide layer formation.

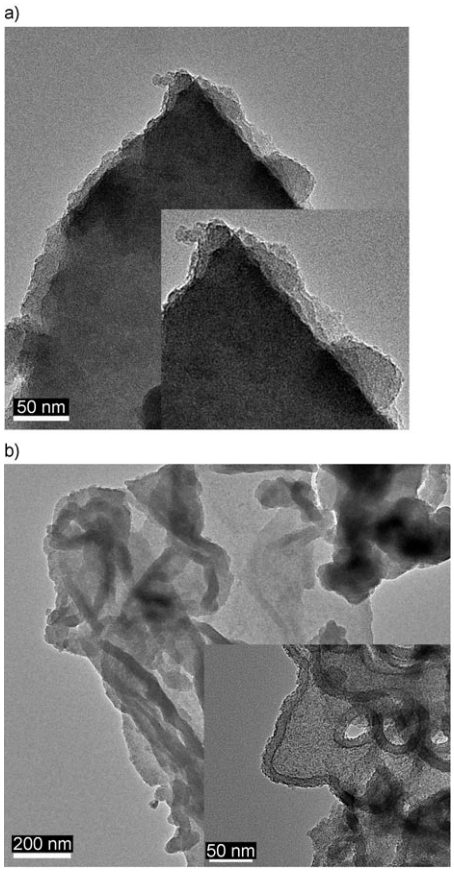

Figure 7. Typical TEM images of TPPhA-Ti. a) Morphology of type 1: plates that have a layered structure; b) morphology of type 2: film-like folded structure that can roll up at the edges.

Indeed, as was shown by the elemental analysis and FT-IR data, the most plausible connectivity pattern is as described in Scheme 2. The X-ray powder pattern has very little detail indicating that the material is poorly ordered and/or that any crystallites which may be present are very small and the diffracted intensity at 2θ values of ~12° and above may possibly be explained by the presence of an amorphous phase which contributes to the intensity at the higher angles. However, the features that are present can be used to provide some, albeit limited, constraints for a molecular model.[16] Thus, in support of the suggested arrangement, a computer-generated and geometrically optimized model comprised of six molecules of TPPhA connected through Ar-$P(O)O_2Ti_2O_2(O)$PAr units shown in Figure 9 was used for an X-ray diffraction simulation. As shown in Figure 6 (dashed line) the simulated pattern is in reasonable agreement with the observed XRD pattern of TPPhA-Ti in the low angle region, nearly matching the positions of the two peaks at 5.8° and 11.2°.[17]

As can be seen from Figure 9, the calculated micropore sizes, have an average diameter of $\approx$15.6 Å. Importantly, this value is also consistent with the calculated pore size, that is, it is within the pore range size of 13.5 ± 4 Å derived using the SF model from the adsorption isotherm (see Figure 3, bottom). The presence in TPPhA-Ti of an amor-

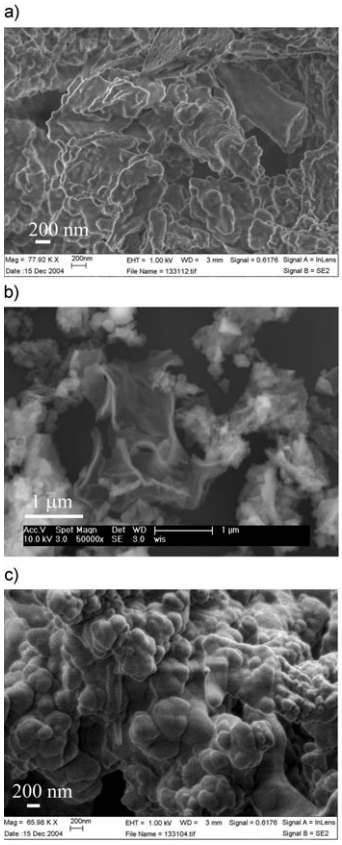

Figure 8. Typical SEM images of the Ti–PD1 specimen; a) lamellar plates; b) folded film structure; c) hemispherical outgrowths.

phous phase impurity can be explained by a random arrangement of the TPPhA molecules with the phosphonic groups bound to only one titanium atom. In this case, the Ti/P ratio and the spectral properties of such a compound and of the regularly arranged molecules in the model are expected to be identical. Indeed, among all the techniques that were used in the structural and spectral characterization of the TPPhA-Ti hybrid material, only XRD, SEM, and, to a lesser extent, TEM gave evidence of structural inhomogeneity.

In order to study the influence of the titanium alkoxide addition rate on the properties of the resulting hybrid compound, neat titanium alkoxide was diluted with dry THF and slowly added by means of a syringe pump to the mechanically stirred solution of tetrakis-1,3,5,7-(4-phosphonatophenyl)adamantane in DMSO. The resulting compound was separated and treated in the same way as was described for the TPPhA-Ti hybrid material (see Experimental Section). It was expected that slow addition of titanium alkoxide would result predominantly in the formation of organophosphonate–titanium films (Figure 8b). However, examination of the sample morphology by means of TEM revealed the formation of spherical particles with an average diameter of ~180–300 nm (Figure 10a). Tilting the grid to different angles (+40 and −40°, respectively) (Figure 10b and c) showed no significant changes in the particle shape and diameter, lending strong support for particle sphericity. Another interesting observation concerns particle edges that appeared to be lamellar (Figure 10a–c); there are several low contrast regions within the particles suggesting that the inside may be hollow and sponge-like.

Energy dispersive X-ray spectroscopic microanalysis (EDS) gives an Ti/P average ratio of 3.4:1 pointing to the fact that nanospheres are composed of the titanium oxide–titanium phosphonate mixture with a predominance of titanium oxide.

Typical high-resolution SEM images are presented in Figure 11 and show nanospheres as nearly the only type of specimen morphology. Some of the nanospheres are broken and one can see their hollow interior (Figure 11b and c; note spheres emphasized with arrows).

A plausible explanation for the formation of spherically shaped particles can be given if we assume that drops of a solution of titanium alkoxide in THF added to a solution of phosphonic acid in DMSO do not immediately disappear but, on the contrary, splinter into many smaller nanosized spheres that become covered with growing layers of the titanium phosphonate polymer which preserves the initial shape of the nanodrops. The process that

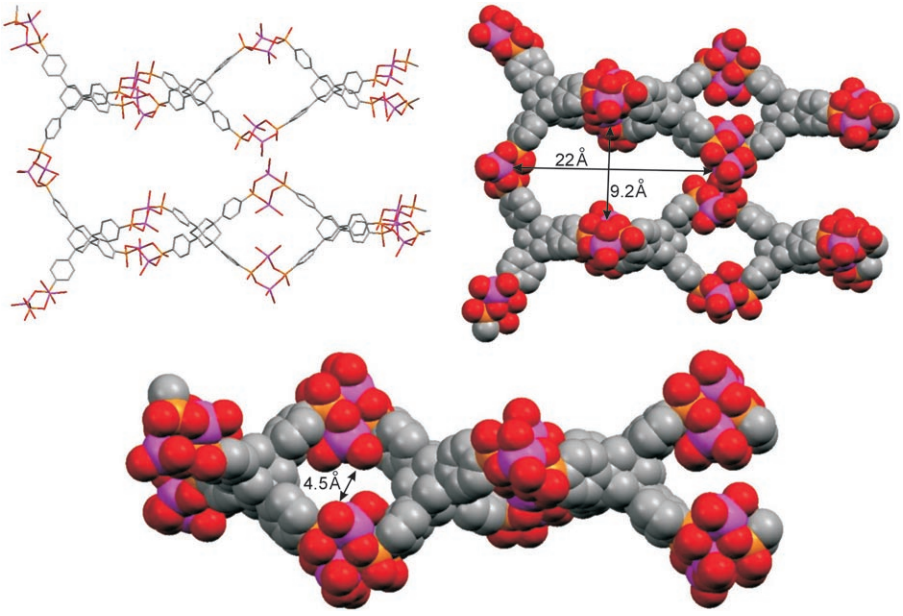

Figure 9. Computer-generated model of the TPPhA-Ti fragment.

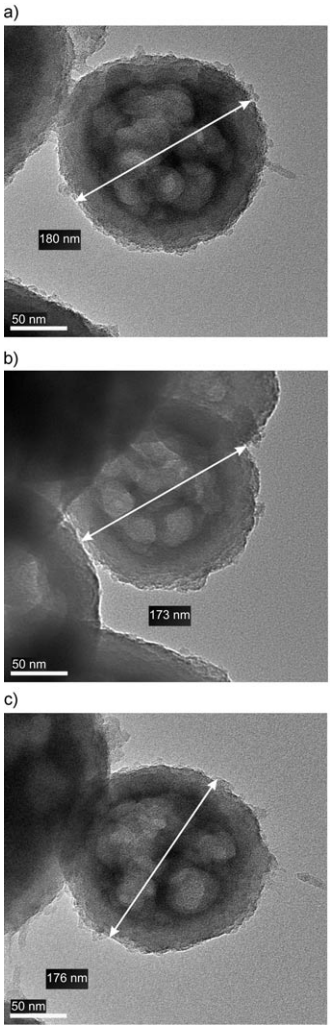

Figure 10. Typical TEM images of the Ti oxide–phosphonate nanospheres: a) tilt angle 0°; b) tilt angle +40°; c) tilt angle −40°.

leads to the formation of the titanium oxide–phosphonate nanospheres has a strong similarity to the interfacial emulsion polymerization technique that has been developed for the hollow CdS[18] (using CS_2/water emulsion) and silica[19] (using an oil/water emulsion) hollow nanosphere synthesis. However, to the best of our knowledge, this is the first time titanium phosphonate nanospheres have been prepared.

One of the interesting potential applications of the nanosphere synthesis can be inclusion of different compounds into the Ti oxide–phosphonate nanosphere wall and interior by dissolving them in the THF/Ti alkoxide mixture that is then added to the solution of organophosphonate in DMSO. This particular application of these new mesoporous materials is currently under study.

Experimental Section

Materials and methods: Titanium(IV) isopropoxide, diethylphosphite, triethylamine, anhydrous benzene and dichlorobis(triphenylphosphine)palladium(II) were obtained from Aldrich and used as received. [Bis(trifluoroacetoxy)iodo]benzene was obtained from Fluka and used as received. DMSO anhydrous $\geq$99.9% grade was received from Aldrich and stored under 4 Å molecular sieves before use. The $^{31}P\{^1H\}$ MAS NMR spectra were measured on a Bruker DSX 300 Avance spectrometer with 4 mm probe head (Bruker) at 121.5 MHz with MAS rate of 5 kHz using a cross-polarization (CP) pulse sequence followed by ^1H high-power decoupling. Chemical shifts are reported as ppm relative to an external 85% phosphoric acid standard. The ^1H NMR spectra were measured on a Bruker Avance 400 spectrometer at 400 MHz in $CDCl_3$ or $[D_6]$DMSO and the chemical shifts are reported as ppm relative to an internal tetramethylsilane standard. $^{13}C\{^1H\}$ NMR spectra were measured on a Bruker Avance 400 spectrometer at 100.6 MHz in $CDCl_3$ or $[D_6]$DMSO solvents. ^{31}P NMR spectra were measured on a Bruker DPX 250 spectrometer at 101 MHz in $CDCl_3$ or $[D_6]$DMSO and the chemical shifts are reported as ppm relative to an external 85% phosphoric acid standard at 300 K with line broadening of 1 Hz. The IR spectrum was measured on a Nicolet Protégé 460 with a sample deposited in the KBr pellet.

TEM and EDS studies: A Philips CM-120 ST transmission electron microscope, operating at 120 kV, was used to observe the morphology of the material. Samples were prepared by dispersing the particles in ethyl alcohol by ultrasonic treatment and then dropping them onto a holey carbon film supported on a copper grid. The samples were stable under electron beam radiation. Energy dispersive spectrometry (EDS) analysis was carried out using an EDAX instrument (Phoenix) equipped with a Si(Li) retractable detector with a super ultra thin window.

SEM studies: A FEI (Philips) XL 30 ESEM-FEG with accelerating voltage of 10 kV and SUPRA 55 VP FEG LEO HR SEM with accelerating voltage of 1.0 kV were used to observe the morphology of the materials. Samples were prepared by dispersing the particles in ethyl alcohol by ultrasonic treatment and dropping them onto silicon slides.

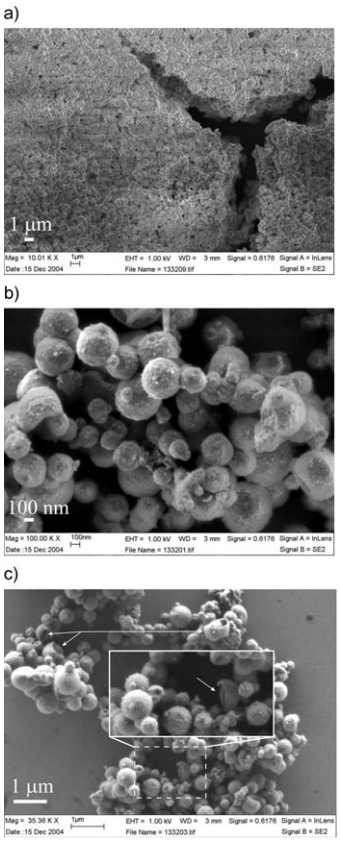

Figure 11. Typical SEM images of the Ti oxide–phosphonate nanospheres.

N_2 sorption studies: Sorption experiments were carried out using Quantachrome Nova 1000 high speed sorption analyzer. Data were analyzed (BET surface–area calculation, BJH and SF pore size distribution) by using NOVAWin software. TPPhA-Ti hybrid material was degassed for 4 h at 100 °C prior measurement. Pore size calculation for determination of mesopore size distribution was conducted from the desorption branch of isotherm using Barrett–Joyner–Halenda method[9] taking in account data points above 0.35P per P_0. Micropore size distribution curve was derived from the adsorption branch of isotherm using Saito–Foley (SF) pore model.[12] N_2 sorption isotherms were measured at least three times and were found reproducible as well as corresponding pore size distribution data. Surface–area calculated using five point nitrogen Brenauer–Emmet–Teller (BET) method[8] gave values of 557, 555 and 614 $m^2 g^{-1}$ over tree consecutive measurements. BET plot presented as an insert in the Figure 2 corresponds to the first of the three area values noted above.

XRD measurements and X-ray diffraction simulation: X-ray powder diffraction patterns were measured in the $\theta/2\theta$ mode using a D-Max/B horizontal goniometer (Rigaku) affixed to a RU200 rotating anode X-ray generator (12 kW, Rigaku) with Cu target ($Cu_{K\alpha}$). The sample was dispersed on a background-free silicon sample holder. Simulation of the X-ray diffraction pattern was carried out using Multibody for Windows software (PCG Software Package 7.2, Graz). The molecular model was input to the program in .pdb (Protein Data Bank) format and the scattering profile calculated using the Debye equation. Geometric optimization of the structural model of TPPhA-Ti hybrid material was accomplished using a semi-empirical PM3 model on Spartan′04 Macintosh software.

Thermal gravimetric analysis: Thermal gravimetric analysis was carried out on Shimadzu DTG-50 analyzer.

Synthesis

Tetrakis-1,3,5,7-(4-diethylphosphonatophenyl)adamantine: Diethyl phosphite (2.48 mL, 19.4 mmol), triethylamine (5 mL) and dichlorobis(triphenylphosphine)palladium(II) (0.02 g, 0.032 mmol) were added under an argon atmosphere to an Ace glass pressure tube containing a solution of tetrakis-1,3,5,7-(4-iodophenyl)adamantane (1 g, 1 mmol) in dry benzene (10 mL). A stirring bar was added and the pressure tube was sealed. The mixture was heated at 80 °C for 72 h with stirring, and then cooled; the precipitated triethylammonium iodide was filtered off. The filtrate was concentrated by evaporation and the residual oil was diluted with cold water (100 mL). The precipitate obtained was filtered, washed twice with water and dried under high vacuum for 72 h. This gave tetrakis-1,3,5,7-(4-diethylphosphonatophenyl)adamantane as a pale-yellow slightly hygroscopic solid (0.75 g, 76 %). The product was sufficiently pure enough to use without further purification. ^{1}H NMR (400 MHz, $CDCl_3$): $\delta = 1.3$ (t, $J = 7$ Hz, 24H), 2.2 (brs, 12H), 4.1 (m, 16H), 7.6 (d, $J = 4$ Hz, 8H), 7.8 ppm (m, 8H); ^{31}P NMR (101 MHz, $CDCl_3$): $\delta = 17.6$ ppm (s); ^{13}C NMR (100.6 MHz, $CDCl_3$): $\delta = 16.26$ (d, J(C,P) = 7 Hz), 39.46, 46.50, 62.08 (d, J(C,P) = 5 Hz), 125.12 (d, J(C,P) = 15 Hz), 126.04 (d, J(C,P) = 234 Hz), 132.06 (d, 10 Hz), 152.98 ppm (d, J(C,P) = 3 Hz); IR (KBr): $\tilde{\nu}$ = 2983, 2931, 2903, 2855, 1603, 1394, 1243, 1130, 1052, 1020, 964, 759, 670 cm^{-1}.

Tetrakis-1,3,5,7-(4-phosphonatophenyl)adamantane: Tetrakis-1,3,5,7-(4-diethylphosphonatophenyl)adamantane (1.7 g, 1.73 mmol) was placed in a round bottom flask and concentrated aqueous solution of hydrogen chloride (150 mL) was added. The mixture was refluxed with vigorous stirring overnight and cooled. A white precipitate was filtered off and quickly transferred to a round bottom flask and dried under high vacuum for 72 h to yield a white slightly hygroscopic powder (1.2 g, 93 %). ^{1}H NMR (400 MHz, [D$_6$]DMSO): $\delta = 2.1$ (brs, 12H), 7.6 ppm (m, 16H); ^{31}P NMR (101 MHz, [D$_6$]DMSO): $\delta = 12$ ppm (s); IR (KBr): $\tilde{\nu}$ = 3448, 2923, 2898, 2852, 1604,1500, 1444, 1396, 1138, 999, 929, 827, 704, 559, 490 cm^{-1}; elemental analysis calcd (%) for $C_{34}H_{36}O_{12}P_4$: C 58.89, H 4.24; found: C 58.69, H 4.04.

Tetrakis-1,3,5,7-(4-phosphonophenyl)adamantane-Ti hybrid material (TPPhA-Ti): Tetrakis-1,3,5,7-(4-phosphonatophenyl)adamantane (1 g, 1.31 mmol) was dissolved in dry DMSO (100 mL) with stirring and neat titanium(IV) isopropoxide (1.56 mL, 5.26 mmol) was added to this solution dropwise. Immediately white precipitate was formed and the reaction mixture was left stirred for two days. The white precipitate was separated by centrifugation, thoroughly washed with H_2O, EtOH, Et_2O and dried under high vacuum for 10 h (0.91 g, 49 %). ^{31}P CP MAS NMR (121.5 MHz, contact time 1 ms): $\delta = 13.4$ ppm; IR (KBr): $\tilde{\nu}$ = 2925, 2854, 1637, 1604, 1396, 1136, 1026, 1001, 1030, 833, 708, 578 cm^{-1}; elemental analysis calcd (%) for $C_{34}H_{36}O_{20}P_4Ti_4 \cdot 14H_2O$: C 31.33, H 4.53, P 9.8; found: C 30.65, H 4.84, P 9.8. The amount of hydrated water was determined by TGA: 18.9 %. Ratio of P/Ti by EDS was 1.09 ± 0.05 for an average of three measurements.

Ti oxide–phosphonate nanospheres: Ti oxide-phosphonate nanospheres were prepared in the same way as described for TPPhA-Ti except titanium(IV) isopropoxide (1.56 mL, 5.26 mmol) was added as a solution in dry THF (10 mL) by means of a syringe pump with the addition rate of 59 μL per min. IR (KBr): $\tilde{\nu}$ = 3392, 2960, 2931, 2856, 1604, 1396, 1261, 1138, 1105, 831, 804, 706, 575 cm^{-1}. Ratio of Ti/P by EDS was 3.4 ± 0.2 for an average of three measurements.

Acknowledgements

This research was supported by the Minerva Foundation and the Helen and Martin Kimmel Center for Molecular Design. We thank Dr. Konstantin Gartzman for SEM and Dr. Shifra Kababya for MAS NMR measurements and Prof. Shimon Vega for helpful discussion on the MAS NMR results. R.N. is the Rebecca and Israel Sieff Professor of Organic Chemistry.

[1] A. Clearfield, Z. J. Wang, *Chem. Soc. Dalton Trans.* **2002**, 2937–2947.
[2] A. Clearfield, *Chem. Mater.* **1998**, *10*, 2801–2810.
[3] A. Vioux, J. le Bideau, P. H. Mutin, D. Leclercq, *Top. Curr. Chem.* **2004**, *232*, 145–174.
[4] a) Z. Wang, J. M. Heising, A. Clearfield, *J. Am. Chem. Soc.* **2003**, *125*, 10375–10383; b) A. Dokoutchaev, V. V. Krishnan, M. E. Thompson, M. Balasubramanian, *J. Mol. Struct.* **1998**, *470*, 191–205; c) O. R. Evans, H. L. Ngo, W. Lin, *J. Am. Chem. Soc.* **2001**, *123*, 10395–10396; d) A. Hu, H. L. Ngo, W. Lin, *Angew. Chem.* **2003**, *115*, 6182–6185; *Angew. Chem. Int. Ed.* **2003**, *42*, 6000–6003; e) A. Hu, H. L. Ngo, W. Lin, *J. Am. Chem. Soc.* **2003**, *125*, 11490–11491; f) A. Hu, H. L. Ngo, W. Lin, *Angew. Chem.* **2004**, *116*, 2555–2558; *Angew. Chem. Int. Ed.* **2004**, *43*, 2501–2504.
[5] P. H. Mutin, G. Guerrero, A. Vioux, *Com. Rendus Chim.* **2003**, *6*, 1153–1164.
[6] G. Alberti, U. Costantino, F. Marmottini, R. Vivani, P. Zappelli, *Angew. Chem.* **1993**, *105*, 1396–1398; *Angew. Chem. Int. Ed. Engl.* **1993**, *32*, 1357–1399.
[7] J. Kim, B. Chen, T. M. Reineke, H. Li, M. Eddaoudi, D. B. Moler, M. O'Keeffe, O. M. Yaghi, *J. Am. Chem. Soc.* **2001**, *123*, 8239–8247.
[8] S. Brunauer, P. H. Emmett, E. Teller, *J. Am. Chem. Soc.* **1938**, *60*, 309–319.
[9] E. P. Barrett, L. G. Joyner, P. P. Halenda, *J. Am. Chem. Soc.* **1951**, *73*, 373–380.
[10] a) J. H. de Boer, B. G. Linsen, T. van der Plas, G. J. Zondervan, *J. Catal.* **1965**, *4*, 649–653; b) J. H. de Boer, B. G. Linsen, T. J. Osinga, *J. Catal.* **1965**, *4*, 643–648; c) B. C. Lippens, J. H. de Boer, *J. Catal.* **1965**, *4*, 319–323.
[11] M. R. Bhambhani, P. A. Cutting, K. S. W. Sing, D. H. Turk, *J. Colloid Interface Sci.* **1972**, *38*, 109–117.
[12] A. Saito, H. C. Foley, *AIChE J.* **1991**, *37*, 429–436.
[13] D. Deniaud, B. Schollorn, D. Mansuy, J. Rouxel, P. Battioni, B. Bujoli, *Chem. Mater.* **1995**, *7*, 995–1000.
[14] G. Guerrero, P. H. Mutin, A. Vioux, *Chem. Mater.* **2000**, *12*, 1268–1272.
[15] a) E. Jaimez, A. Bortun, G. B. Hix, J. R. Garcia, J. Rodriguez, R. C. T. Slade, *J. Chem. Soc. Dalton Trans.* **1996**, 2285–2292; b) G. Guerrero, P. H. Mutin, A. Vioux, *Chem. Mater.* **2001**, *13*, 4367–4373.

[16] We have carried out the molecular modeling assuming tetracoordinated titanium; hexacoordinated titanium could also be considered. It may also be possible to consider additional models that would fit the x-ray diffraction and pore size measurements. We will consider this matter more carefully in the future though ^{13}Al MAS NMR experiments using analogously prepared aluminumphosphonates.
[17] A reviewer commented on the large FWHN values used to fit the experimental data. However, one should realize that the large FWHM of the intensity maxima in the calculated scattering pattern derives naturally from the small number of repeating units used in the model and not from any artificially imposed line widths.
[18] J. Huang, Y. Xie, B. Li, Y. Liu, Y. Qian, S. Zhang, *Adv. Mater.* ***2000****, 12*, 808–811.
[19] S. Schacht, Q. Huo, I. G. Voigt-Martin, G. D. Stucky, F. Schuth, *Science* **1996**, *273*, 768–771.

Received: September 15, 2005
Published online: February 21, 2006

